Back

OBSERVATION OF SOLAR AND LONG-WAVE RADIATION FIELDS IN URBAN CANYON BY USING A CUBIC RADIOMETER

Yasuto Nakamura*, Makihiko Tsujihara*, Harumi Kagawa**
*Prefectural University of Kumamoto, Kumamoto, Japan; **The University of Kitakyushu, Kitakyushu, Japan

Abstract

Observation of solar and long-wave radiation fields was carried out using a cubic radiometer at the eight points in the urban area including canyon in a clear day on March. The measurement was practiced three times of morning, afternoon and evening with 10 minutes recording at each point. The radiation fields from the viewpoint of energy transfer are analyzed for radiation fluxes incident on the horizontal plane. From the viewpoint of bioclimate, the radiation fields are evaluated with the equivalent air temperature, the operative temperature and the SET*.

Key words: net radiation flux, equivalent air temperature, cubic radiometer

1. INTRODUCTION

In urban areas more or less a field of vision to the sky narrows, particularly the sky view factor in the urban canyon is considerably restricted. In the canyon sunny and shady areas are formed and solar and long-wave radiation flux flow is complex due to various objects such as buildings, facilities, trees, etc. However, to grasp the real state of radiation fields in the urban canyon is earnestly requested for understanding urban climate. A cubic radiometer is effective as a means for obtaining radiation fields indoors including both solar radiation and long-wave radiation, that is already confirmed in reference (Nakamura, 1983; Kagawa, et al., 2003). In this paper the cubic radiometer is extended to use outdoors in order to grasp the characteristics of radiation fields in the urban canyon.

2. STRUCTURE AND CALIBRATION OF A CUBIC RADIOMETER

2.1. Structure of a cubic radiometer

A cubic radiometer is made of six independent radiant flux detectors on the surface of a cube. Each radiant flux detector is a plate like detector of 10 cm x 10 cm square and is able to measure simultaneously and separately solar and long-wave radiation fluxes incident on the surface of the detector. The central 3 cm x 3 cm square of the detector is an area of sensor, which consists of three kinds of element with mutually different surfaces from the viewpoint of radiation. The substance of the element is a heat flow meter. In measurement using the radiant flux detector, data of a surface temperature of the element and three electric motive forces of elements are collected (Nakamura, 1983). The cubic radiometer is supported by four pods 1 meter high above the ground, which is chosen as a central height corresponding to a standing person. Usually, data are recorded with 1 minute mean of 6 seconds interval collecting through a data recorder.

2.2. Principle of measurement

With respect to the three elements type of sensor in each detector, a balance between a heat budget equation for the surface of the 2nd element and one of the 1st element is made, and another balance between a heat budget equation for the 3rd element and one of the 1st element is made. Then, combining these balances is able to bring equations to get fluxes of solar and long-wave radiation incident on the detector, which are as follows;

$$J = (\mathrm{E}_{12}\, Q_{13} - \mathrm{E}_{13}\, Q_{12}) / (\mathrm{A}_{13}\, \mathrm{E}_{12} - \mathrm{A}_{12}\, \mathrm{E}_{13}) \tag{1}$$

$$\sigma T_r^{\,4} = (\mathrm{A}_{13}\, Q_{12} - \mathrm{A}_{12}\, Q_{13}) / (\mathrm{A}_{13}\, \mathrm{E}_{12} - \mathrm{A}_{12}\, \mathrm{E}_{13}) + \sigma T_1^{\,4} \tag{2}$$

where

$$Q_{12} = (\mathrm{K}_1 V_1 + \mathrm{K}_2 V_2) / (1 - \mathrm{C}_{12}\, u^{1/2}) \tag{3}$$

$$Q_{13} = (\mathrm{K}_1 V_1 + \mathrm{K}_3 V_3) / (1 - \mathrm{C}_{13}\, u^{1/2}) \tag{4}$$

where

J : incident solar radiation [$\mathrm{Wm^{-2}}$], $\sigma T_r^{\,4}$: incident long-wave radiation [$\mathrm{Wm^{-2}}$],
T_1 : surface temperature of the 1st element [K], u : surrounding air velocity [$\mathrm{ms^{-1}}$],

* *Corresponding author address*: Yasuto Nakamura, Faculty of Environmental and Symbiotic Sciences, Prefectural University of Kumamoto, Kumamoto 862-8502, Japan; e-mail: ynaka@pu-kumamoto.ac.jp

K : reciprocal sensitivity [Wm^{-2}/mV], E : effective absorptivity for long-wave radiation [ND],
A : effective absorptivity for solar radiation [ND], C : corrective constant for air velocity [$(ms^{-1})^{-1/2}$],
V : electric motive force [mV], σ : the Stefan-Boltzmann constant [$Wm^{-2}K^{-4}$].

The single suffix 1,2,3 respectively implies the 1st, 2nd, 3rd element of the sensor and the double suffix 12 or 13 implies a relation between the 1st element and the 2nd or 3rd element.

2.3. Calibration of the cubic radiometer

In advance, the reciprocal sensitivity of the element K_i (i=1,2,3) was determined by comparing the conductive heat flow of the element with that of the standard plate with the exact thermal conductivity. The corrective constant for air velocity C_{1j} (j=2,3) was theoretically conducted. The calibration of the effective absorptivity for both long-wave radiation and solar radiation, E_{1j} and A_{1j}, were settled for the horizontal plane outdoors. At first, in the night time without solar radiation, the value of E_{1j} was determined on the comparison with the observation of long-wave radiation by a pyrgeometer with silicon dome as the standard. Secondly, in the daytime the A_{1j} was set using the fixed E_{1j} on the observation by both a pyranometer and a pyrgeometer as the standard (Nakamura, et al., 2003).

3. PRACTICE OF OBSERVATION

3.1. Observation site

The observation site was the campus of our university. Eight points were chosen accounting the diversity of sky view factor, ground material, sunny or shady, and others. Observation points were as follows Table 1. The value of sky view factor [ND] was estimated on the photo taken with a fish eye lens.

Table 1 Observation point and surrounding feature

Point	A	B	C	D	E	F	G	H
Location	open space	pavement	court center	court near wall	street canyon	court parking	parking lot	parking lot
S.V.factor	0.895	0.673	0.748	0.559	0.405	0.755	0.948	0.913
Ground material	tile	permea-ble tile	grass	grass shady	asphalt shady	asphalt	asphalt	grass concrete

3.2. Method of observation

A series of observation was practiced three times in a clear day on 26 March 2003; morning, afternoon and evening. An observation interval at each point was 10 minutes. The time required from the point A through H was about 2 hours. In addition to the cubic radiometer, instruments for measuring air temperature, air velocity, humidity, and globe temperature were used. Further, at the top of a near building, solar radiation and atmospheric radiation were measured by a pyranometer and a pyrgeometer, which were the same as used in the calibration.

4. RESULTS OF OBSERVATION

4.1. Radiation flux for horizontal plane

Table 2 shows results of radiation flux for horizontal plane obtained in the observation. 'Sol. incoming' is solar radiation incident on the upper detector of the cube and 'Sol. outgoing' is equal to that incident on the under detector of the cube. And 'Net radiation' implies the net radiation flux in the direction from upper to under. The day of the observation was clear and cloudless from the morning to the evening.

Table 2 Radiation flux for horizontal plane [Wm^{-2}], morning and afternoon

Point	A	B	C	D	E	F	G	H
Morning (09:30 – 11:29)								
Time	09:30 –	09:44 –	10:02 –	10:15 –	10:32 –	10:48 –	11:06 –	11:19 –
Sol. incoming	589	613	650	101	167	788	847	848
Sol. outgoing	113	70	131	4	40	102	98	154
Sol. Net	476	543	519	97	127	686	749	694
L-w. incoming	263	296	299	313	335	315	304	317
L-w. outgoing	414	416	428	375	394	456	489	452
L-w. net	-151	-120	-129	-62	-59	-141	-185	-135
Net radiation	325	423	390	35	68	545	564	559

Afternoon (13:30 – 15:22)								
Time	13:30 –	13:46 –	13:59 –	14:12 –	14:26 –	14:41 –	14:59 –	15:12 –
Sol. incoming	808	816	795	106	188	679	659	611
Sol. outgoing	146	123	153	12	18	95	73	113
Sol. Net	662	693	342	94	170	584	586	498
L-w. incoming	322	335	326	326	364	318	293	288
L-w. outgoing	515	518	468	388	458	514	527	458
L-w. net	-193	-183	-142	-62	-94	-196	-234	-170
Net radiation	469	510	200	32	76	388	352	326

4.2. Equivalent air temperature for radiation effect

With regard to analysis of bioclimate, equivalent air temperature (Nakamura, 1983) was used instead of mean radiant temperature. The equivalent air temperature is to convert the effect of radiation on the human body to rise in air temperature, in which there are two effects of solar and long-wave radiation. The operative temperature is a sum of the air temperature and each equivalent air temperature, that is as follows (Nakamura, 1983);

$$T_o = T_a + t_{el} + t_{es} \tag{5}$$

where

T_o : operative temperature on the human body [K], T_a : surrounding air temperature [K],
t_{el} : equivalent air temperature for long-wave radiation on the human body [deg.C],
t_{es} : equivalent air temperature for solar radiation on the human body [deg.C].

The equivalent air temperature for long-wave radiation is related to the mean radiant temperature and that for solar radiation is expressed using the flux of solar radiation. That is;

$$t_{el} = [\, h_r / (h_r + h_c) \,] \; (T_m - T_a) \tag{6}$$

$$t_{es} = [\, \alpha \, (A_r / A_D) / (h_r + h_c) \,] \; J_m \tag{7}$$

where

h_r : radiative heat transfer coefficient on the human surface [$Wm^{-2}K^{-1}$],
h_c : convective heat transfer coefficient on the human surface [$Wm^{-2}K^{-1}$],
α : solar absorptivity on the human surface [ND], A_r/A_D : effective radiation area factor [ND],
T_m : mean radiant temperature [K], J_m : mean solar radiation incident on the human body [Wm^{-2}].

Table 3 shows the equivalent air temperature estimated for each surface of the cube and the surrounding air temperature in the morning. In the equation (6) and (7), values such as h_r, h_c, A_r, A_D, and α are determined, for instance, by seeing a reference (Parsons, 2003). As for the coefficient, the following approximate and reasonable values were used; $[h_r/(h_r+h_c)] = 0.5$ and $[\alpha(A_r/A_D)/(h_r+h_c)] = 0.05$. Because, h_r=4.7, h_c=4.7, α=0.6 and (A_r/A_D)=0.77 for a standing person. Mean radiant temperature T_m and mean solar radiation J_m defined on the human body are converted to plane radiant temperature (Parsons, 2003) T_r and solar radiation flux J on each surface of the cube. The number 1 to 6 indicates respectively in order up, front, right, back, left, and down surface of the cube. In the observation, the number 1 was always pointed to a direction near the north.

Table 3 Equivalent air temperature and air temperature [deg.C], morning

Point	A	B	C	D	E	F	G	H
Time	09:30 –	09:44 –	10:02 –	10:15 –	10:32 –	10:48 –	11:06 –	11:19 –
Long-wave radiation t_{el}								
No.1	-12.1	-8.7	-8.6	-8.6	-4.9	-7.7	-8.8	-7.7
No.2	-1.9	0.9	-0.4	-2.5	-1.3	1.0	0.7	-0.7
No.3	-2.8	-1.7	-2.5	-2.3	-0.3	-3.8	-3.4	-4.5
No.4	-2.4	-3.0	-1.3	-1.8	-0.5	-0.5	-0.3	-2.0
No.5	-2.0	1.5	0.3	-2.6	1.8	0.4	0.5	-1.0
N0.6	3.6	3.4	4.0	-0.6	0.9	5.5	8.3	5.0
Solar radiation t_{es}								
No.1	29.5	30.7	32.5	5.1	8.4	39.4	42.3	42.4
No.2	5.2	6.3	7.5	3.5	2.9	5.4	7.1	7.9
No.3	26.4	21.5	22.3	2.8	1.8	15.4	14.9	13.1
No.4	22.6	20.9	24.4	2.0	7.3	24.8	28.8	29.2
No.5	5.1	5.3	5.5	2.5	5.6	5.6	7.5	8.9
N0.6	5.6	3.5	6.5	0.2	2.0	5.1	4.9	7.7
Air temp t_a	12.1	12.8	13.5	13.3	13.8	15.3	15.0	15.7

5. DISCUSSION

To remove the trend of data of both the ascent and the descent following the passage of the observation, the mean of data in the morning and in the afternoon is used in the analysis at each point. Except the points D and E because of low value of the sky view factor and to be shady, it is found that the feature of the ground materials is separated in two groups. The low solar reflectivity group of B, F and G holds high values of the net flux of solar radiation because of the low solar outgoing flux. Therefore solar absorptivity increases. On the other hand, according to the high net solar radiation, the net flux of all radiation is also high. Thus, the temperature of ground surface rises and the outgoing flux of long-wave radiation becomes high. The high solar reflectivity group of A, C and H is entirely vise versa. In the urban area with the sky view factor larger than 0.673, use of the high solar reflectivity material is recommended as the ground surface to reduce urban heating.

Figure 1 shows results of air temperature, equivalent air temperature, operative temperature and SET*. The effect of solar radiation on the human body outdoors in the daytime on March in spring is remarkable, because of the high equivalent air temperature for solar radiation up to 15 degree C compared with the air temperature lower than 20 degree C. Usually in the hot environment, the SET* is indicated lower than the operative temperature due to evaporation heat loss. Nevertheless, the SET* in the afternoon except the point D and E reaches to 28 degree C and increases over the indoor thermal comfort limit of 26 degree C. The difference of the effect of the sun and the shade is also marked.

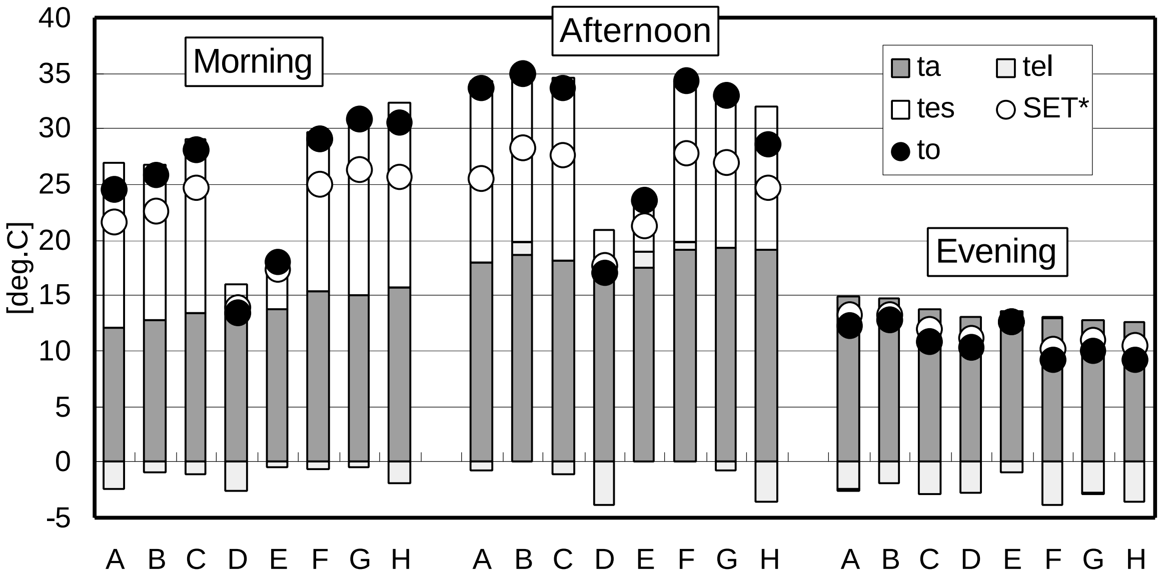

Fig.1 Air temperature t_a, Equivalent air temperature t_e, Operative temperature t_o and SET*

6. CONCLUSION

The cubic radiometer makes it possible to measure simultaneously and separately solar and long-wave radiation fluxes incident on six surfaces of the small cube, which are elements of the radiation fields. The analysis for the horizontal plane based on the observation was performed. The result made clear the remarkable difference of the net incoming radiation flux between the shade and the sun in the urban area in the daytime. As an explanation of the radiation fields for the human body, the equivalent air temperature has been found to be reasonable and able to understand the effect of the surrounding radiation, because of the description with the same measure as the air temperature and the operative temperature.

References

Nakamura, Y., 1983, Measurement of thermal radiation fields on occupied space in a room using the cubic radiant flux detector and personal computer, *The 4th Int. Symp. Use. Comp. Env. Eng. Build.*, 66-71

Nakamura, Y., Tsujihara, M., and Kagawa, H., 2003, Calibration of the cubical radiometer and its application to measurement of indoor thermal radiation fields, Part 1 Calibration, *Proc. AIJ Kyushu Chapter Architectural Research Meeting,* **42**, 253-256

Kagawa, H., Nakamura, Y., Tsujihara, M., and Ishihara, O., 2003, Calibration of the cubical radiometer and its application to measurement of indoor thermal radiation fields, Part 2 Application, *Proc. AIJ Kyushu Chapter Architectural Research Meeting,* **42**, 257-260

Parsons, K., 2003, Human Thermal Environments, 2nd ed., Taylor & Francis.